remote sensing

Article

A Laser-Induced Breakdown Spectroscopy Experiment Platform for High-Degree Simulation of MarSCoDe In Situ Detection on Mars

Zhicheng Cui [1], Liangchen Jia [1], Luning Li [2], Xiangfeng Liu [2], Weiming Xu [1,2], Rong Shu [1,2] and Xuesen Xu [1,2,*]

1 School of Physics and Optoelectronic Engineering, Hangzhou Institute for Advanced Study, University of Chinese Academy of Sciences, Hangzhou 310024, China; cuizhicheng20@mails.ucas.ac.cn (Z.C.); jialiangchen20@mails.ucas.ac.cn (L.J.); xuwm@mail.sitp.ac.cn (W.X.); shurong@mail.sitp.ac.cn (R.S.)

2 Key Laboratory of Space Active Opto-Electronics Technology, Shanghai Institute of Technical Physics, Chinese Academy of Sciences, Shanghai 200083, China; liluning@mail.sitp.ac.cn (L.L.); liuxiangfeng@mail.sitp.ac.cn (X.L.)

* Correspondence: xuxuesen@ucas.ac.cn

Abstract: The Zhurong rover of China's Tianwen-1 mission started its inspection tour on Mars in May 2021. As a major scientific payload onboard the Zhurong rover, the Mars Surface Composition Detector (MarSCoDe) instrument adopts laser-induced breakdown spectroscopy (LIBS) to detect and analyze the chemical composition of Martian materials. This paper introduces an experimental platform capable of establishing a simulated Martian atmospheric environment, in which a duplicate model of the MarSCoDe flight model is placed. In the simulated environment, the limit vacuum degree can reach 10^{-5} Pa level, the temperature can change from −190 °C to +180 °C, and different gases can be filled and mixed according to desired proportion. Moreover, the sample stage can move along a track inside the vacuum chamber, enabling the detection distance to vary from 1.5 m to 7 m. Preliminary experimental results indicate that this platform is able to simulate the scenario of MarSCoDe in situ LIBS detection on Mars well.

Keywords: Tianwen-1 mission; MarSCoDe; laser-induced breakdown spectroscopy (LIBS); simulated Martian environment

Citation: Cui, Z.; Jia, L.; Li, L.; Liu, X.; Xu, W.; Shu, R.; Xu, X. A Laser-Induced Breakdown Spectroscopy Experiment Platform for High-Degree Simulation of MarSCoDe In Situ Detection on Mars. *Remote Sens.* **2022**, *14*, 1954. https://doi.org/10.3390/rs14091954

Academic Editors: Lin Li, Yuanzhi Zhang and Shengbo Chen

Received: 15 March 2022
Accepted: 17 April 2022
Published: 19 April 2022

1. Introduction

In China's Tianwen-1 Mars exploration mission, the Tianwen-1 probe successfully landed on the Martian surface in May 2021, with the landing position in southern Utopia Planitia (25.06°N, 109.92°E) [1], near the landing site of NASA's Viking 2 probe. Thereafter, the Zhurong rover of the Tianwen-1 probe started its inspection tour on Mars.

As a major scientific payload onboard the Zhurong rover, the Mars Surface Composition Detector (MarSCoDe) instrument can implement in situ detection of the Martian surface materials. Adopting laser-induced breakdown spectroscopy (LIBS), short-wave infrared spectroscopy (SWIR), and micro-imaging [2], MarSCoDe is expected to perform identification/classification of Martian soils and rocks, and carry out quantitative determination of the element contents in those materials as well [3,4].

The atmospheric environment of Mars is considerably different from that of our Earth. Specifically for Utopia Planitia, the average surface temperature can change from approximately 160 K (Martian winter) to 240 K (Martian summer) [5], and the highest temperature in Martian summer can reach about 260 K [6], showing consistency with the temperature data reported by Viking 2 probe [7]. As for the air pressure, Viking 2 measurements reveal that the daily average pressure can vary from about 7.5 mbar to 10 mbar throughout the Martian year [8]. Due to the great differences in temperature and air pressure between Mars and Earth, one can hardly directly exploit the LIBS database based on ordinary laboratory environments to assist the analysis of the LIBS spectra from in situ detection on Mars. In order to address this issue, several institutes engaged in planetary science research in the world have established specific facilities to simulate the Martian atmospheric environment.

A group at Washington University in St. Louis has developed a planetary environment and analysis chamber (PEACh) [9], in which several detection techniques can be implemented, such as LIBS, Raman spectroscopy, near-IR reflectance spectroscopy, micro-imaging, etc. The ChemCam team has also developed a Martian Chamber to simulate the Martian atmospheric environment, and collected LIBS spectra from various targets involving 32 elements by a laboratory model of ChemCam [10]. Shandong University in China has designed a Mars environment chamber, which is used to make preparations for the Tianwen-1 Mars mission, such as spectral database construction and chemometrics model development [11].

There are also some other similar facilities in the world, such as a large planetary simulation chamber called Andromeda in the Arkansas-Oklahoma Center for Space and Planetary Science [12], a versatile environmental simulation chamber located in Madrid, Spain [13], and so forth.

For the various existing planetary environment simulation facilities mentioned above, a common feature is that only the target samples could be placed in the vacuum chamber when the experiments are implemented, while the detection instruments are still in the normal air environment. As a result, both the excitation source (e.g., the laser) and the signal light (e.g., the laser-induced plasma radiation) have to pass through the specific transmission window, hence leading to the distortion of the final signals received by the detector.

In order to better utilize the LIBS data from MarSCoDe in situ detection on Mars, we have established a LIBS experimental platform which is capable of simulating the Martian atmospheric environment. The laser-induced breakdown spectroscopy experiment platform contains two parts, i.e., an experiment platform for Martian environment simulation, and a MarSCoDe laboratory model which is nearly identical to the genuine MarSCoDe flight model. Aside from the usual features such as high vacuum degree and wide temperature variation range, our facility has a distinctive merit, i.e., a remarkably large volume. Not only the target samples, but also the LIBS instrument, can be put into the vacuum chamber when the LIBS measurements are carried out. The LIBS instrument employed here is a duplicate model of the MarSCoDe model launched in the Tianwen-1 mission. As such, the real scenario of MarSCoDe in situ detection on Mars can be well simulated. In the following, we will provide a brief introduction to the MarSCoDe laboratory model (Section 2), elucidate the technical aspects of the experimental platform for Martian environment simulation (Section 3), and then some results for technical specification verification will be presented (Section 4). After that, we will show and discuss some preliminary results of the LIBS experiments conducted by this facility (Section 5), followed by the conclusions section (Section 6).

2. The MarSCoDe Laboratory Model

The MarSCoDe instrument is one of the six major scientific payloads onboard the Zhurong rover. Equipped with the technical functions of LIBS, SWIR, and micro-imaging, MarSCoDe is expected to detect and analyze the chemical compositions in the soils and rocks on the Martian surface. To achieve high-degree simulation of the field detection on Mars, we employ a MarSCoDe laboratory model for the experiment platform, with its technical specifications nearly identical to the real MarSCoDe instrument.

The appearance of the MarSCoDe laboratory model is shown in Figure 1a. In Figure 1b, we illustrate the main components of the MarSCoDe instrument suite. Specifically, it contains six units: a 2D pointing mirror unit and an optical head unit outside the rover cabin, a LIBS and SWIR spectrometer unit and a master controller unit inside the cabin, LIBS calibration targets, and SWIR calibration targets. The 2D pointing mirror unit enables the laser to point to the target and receive the emission light from it. The optical head unit is an integration of telescopic and receiving optics, a set of autofocus mechanism, a laser head, and micro-imaging camera electronics. The received LIBS signals and SWIR signals are imported into the spectrometer through two optical fibers. The spectrometer unit inside the cabin integrates laser driver electronics, the LIBS spectrometer, the SWIR spectrometer, and related electronics. After entering the spectrometer unit, the LIBS signals will be divided into three spectral channels by a demultiplexer, and received by a three-channel spectrometer module. The reflected solar spectra from the detected target will be collected by the SWIR spectrometer, with the receiving band being 850 to 2400 nm. The master controller electronics unit controls the operation of MarSCoDe and provides all the necessary power supply voltage. Some main technical specifications of the MarSCoDe instrument are displayed in Table 1.

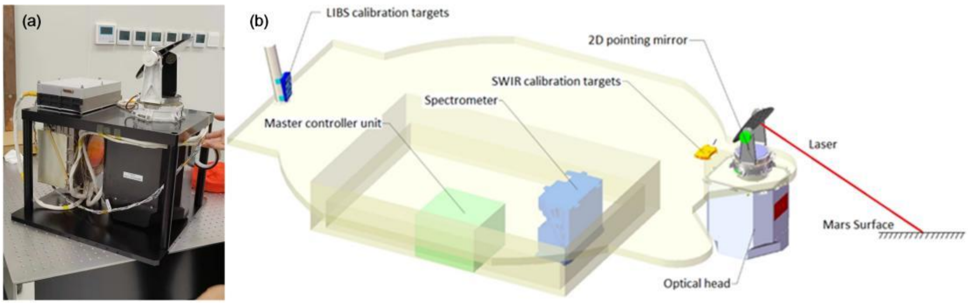

Figure 1. (**a**) Appearance of the MarSCoDe laboratory model. (**b**) Schematic diagram of the MarSCoDe instrument suite onboard the Zhurong rover.

Table 1. Main technical specifications of the MarSCoDe instrument.

Unit	Parameter	Value
LIBS and micro-imaging camera unit	Detection distance	1.6–5 m, up to 7 m
	LIBS sampling interval	0.067 nm @240–340 nm 0.132 nm @340–540 nm 0.203 nm @540–850 nm
	Laser repetition rate	1 Hz, 2 Hz, 3 Hz
	Laser wavelength	1064 nm
	Micro-image	64 × 64, 1024 × 1024 optional
	Micro-image resolution	62.5 µrad @ 2 m 72.0 µrad @ 5 m
SWIR unit	Spectral range	850–2400 nm
	Spectral resolution	3–12 nm
	Bands	321 bands, 64 bands optional @ 5 nm sampling interval
	Field of view	36.5 mrad
2D pointing mirror unit	Pointing range	Pitch: −21°–+199° Azimuth: −59°–+32°
	Pointing accuracy	Pitch 0.133°, Azimuth 0.076°
	Pointing stability	Pitch 0.035°, Azimuth 0.043°

The comprehensive introduction of the MarSCoDe instrument with more technical details can be found in [3]. Since the MarSCoDe laboratory model mentioned above has nearly identical technical performance as the MarSCoDe onboard the Zhurong rover, the combinative use of the duplicate model and the simulated Martian environment can ensure the high-degree simulation of the actual LIBS detection on Mars.

3. The Experiment Platform for Martian Environment Simulation

The experiment platform for Martian environment simulation was developed by Shanghai Institute of Technical Physics, Chinese Academy of Sciences, and is located in

Hangzhou Institute for Advanced Study, University of Chinese Academy of Sciences. The whole facility generally comprises an instrument cabin (also called vacuum jar), a sample cabin, a sample import chamber (also called pre-pumping sample chamber), a 3D vacuum stage, a vacuum pumping system, a temperature control system, an atmosphere simulation system, a measurement and control system, and other auxiliary devices. The schematic diagram and a photograph of the facility are shown in Figure 2a,b, respectively.

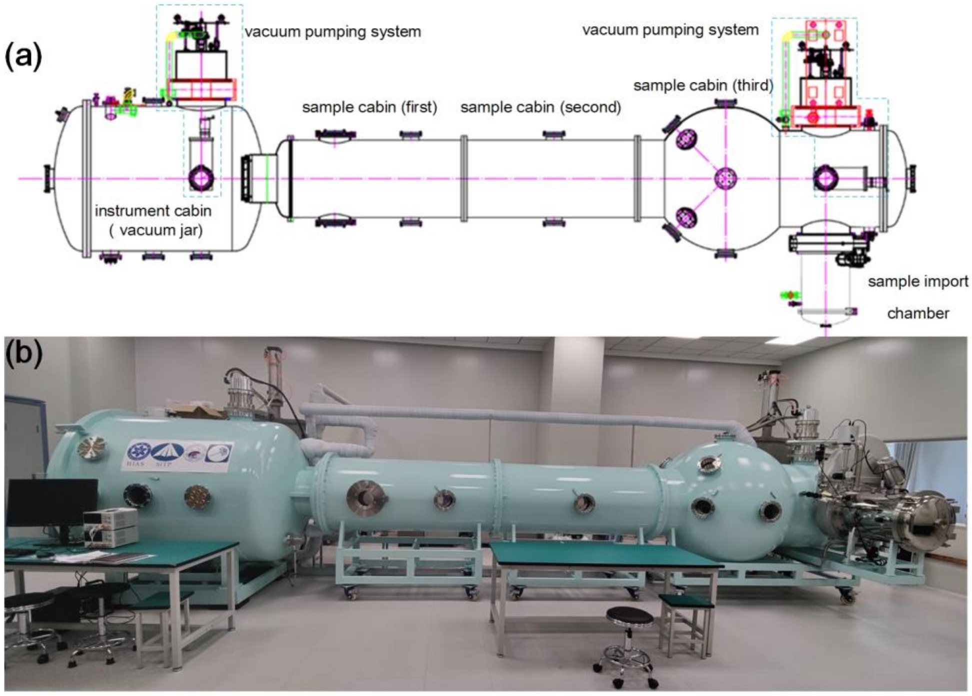

Figure 2. Schematic diagram (**a**) and photograph (**b**) of the facility for Martian atmospheric environment simulation, which is located in Hangzhou, China.

The different modules of the whole facility, the units included in each module, and their corresponding functions are described in Table 2, with further details elucidated in the following subsections.

3.1. Vacuum Chamber

The vacuum chamber includes an instrument cabin (vacuum jar), a sample cabin, a sample import chamber (pre-pumping sample chamber), a sample delivery device, and a 3D vacuum stage.

Adopting horizontal structure, the instrument cabin is made of stainless steel, with the internal diameter 1500 mm, the wall thickness 8 mm, and the straight section length 1500 mm. The instrument cabin is shown in Figure 3a. Inside the instrument cabin, there is a cold plate, which is made of oxygen-free copper and used for bearing the LIBS instrument (MarSCoDe duplicate model). The cold plate has a plane size of 700 mm $\times$ 1000 mm and a bearing capacity of over 100 kg. When placed on the cold plate, the MarSCoDe laboratory model is connected to the power supply and the inspection module through cables. A photograph of the MarSCoDe laboratory model inside the instrument cabin is shown in Figure 3b.

Table 2. The modules and included units of the facility and their corresponding functions.

Module	Units in the Module	Function Description
Vacuum chamber	instrument cabin (vacuum jar)	holding the LIBS instrument (MarSCoDe laboratory model)
	sample cabin	holding the target samples
	sample import chamber (pre-pumping sample chamber)	implementing sample (batch) replacement without exposing the sample cabin to the air
	sample delivery device	realizing efficient sample delivery
	3D vacuum stage	realizing the rotation and horizontal/vertical translation of the samples in the sample cabin
Vacuum pumping system	oilless dry pump	join in from the beginning, i.e., the primary pumping, reducing the cabin pressure to 10^{-1} Pa level
	magnetic suspension molecular pump	join in when the secondary pumping starts, reducing the cabin pressure to 10^{-4} Pa level
	cryogenic pump	join in when the tertiary pumping starts, reducing the cabin pressure to 10^{-5} Pa level
Temperature control system	heating system liquid nitrogen cooling system	realizing a temperature variation range of −190 °C–+180 °C
Atmosphere simulation system	gas filling and mixing unit	simulating a desired atmospheric environment
	quadrupole mass spectrometer	monitoring the gas composition and proportion in the simulated environment in real-time
Measurement and control system	computer central control unit	visualizing and managing the various parameters of the facility
	vacuum measuring instrument	monitoring the air pressure in the simulated environment in real-time
	temperature inspection instrument	monitoring the temperatures of specific positions in real-time

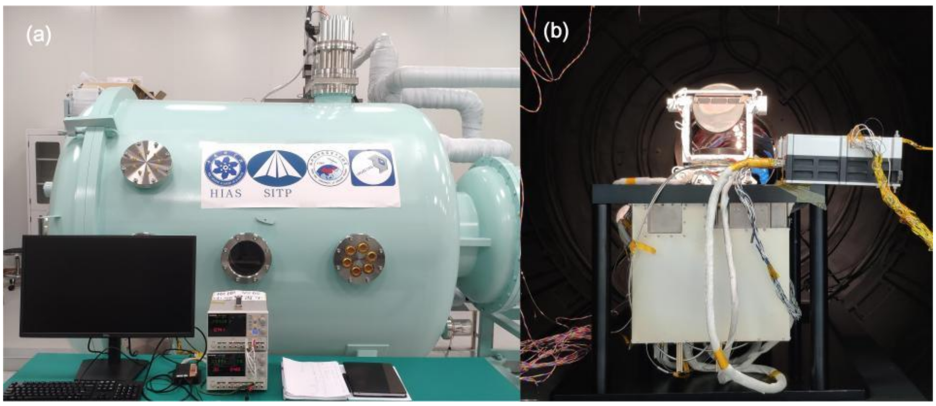

Figure 3. (**a**) Appearance of the instrument cabin. (**b**) Photograph of the MarSCoDe laboratory model inside the instrument cabin.

The sample cabin has a three-section structure, with two cylindrical sections and one nearly spherical section. Each of the first two sections has an internal diameter of 800 mm and a straight section length of 1800 mm. The third section consists of three parts, i.e., a cylinder part (800 mm diameter and 300 mm length), a nearly spherical part (1500 mm diameter and 1166 mm length), and another cylinder part (1000 mm diameter and 1100 mm length). The wall thickness of each of the three sections is 6 mm. Inside the sample cabin, there is a track and a 3D vacuum stage. To conduct LIBS measurements, we can place the target samples on a sample plate (with 16 sample seats) and fix them by spring clips, as shown in Figure 4a. Then, the sample plate can be put onto the 3D vacuum stage, which is displayed in Figure 4b. Through the vertical translation of the stage, the height of the sample plate can be adjusted from 0 mm to 50 mm (sub-millimeter positioning accuracy). Moreover, the stage can move horizontally along the track, thereby allowing a LIBS detection distance ranging from 1.5 m to 7 m (sub-millimeter positioning accuracy). Moreover, different target samples can be detected in turn through the rotation of the stage, with the rotation angle varying from 0° to 340° and the accuracy better than 0.1°. Note that although there are 16 samples seats in the sample plate, only 15 samples can be detected within one batch since the maximum rotation angle is 340° rather than 360°.

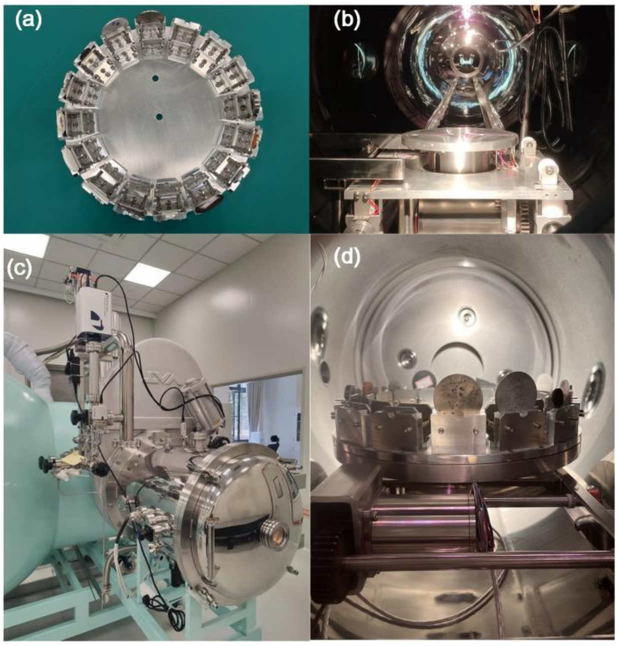

Figure 4. (**a**) The sample plate with 16 sample seats. (**b**) The 3D vacuum stage and the track. (**c**) The external appearance of the sample import chamber. (**d**) The internal appearance of the sample import chamber, with the sample plate placed on the sample delivery device.

After collecting the LIBS spectra from one batch of samples (15 samples), we may need to take out the sample plate and replace this batch with another batch. The sample import chamber is designed to avoid exposing the sample cabin to the air in the laboratory when we implement the replacement. The sample import chamber has a horizontal structure, with a 500 mm diameter and a 620 mm length, and its appearance is shown in Figure 4c. A moderate vacuum with a pressure of approximately 10^{-1} Pa can be achieved in the sample import chamber, which is linked to the oilless dry pump able to implement pre-pumping. The connectivity between the sample import chamber and the sample cabin is controlled by a pneumatic gate valve. Driven by an electric motor, the sample delivery device can import the sample plate into the sample cabin, as illustrated in Figure 4d.

3.2. Vacuum Pumping System

The vacuum pumping system includes two identical pump sets, with each set comprising three kinds of pumps, i.e., an oilless dry pump (HANBELL PS-160), a magnetic suspension molecular pump (SHIMADZU TMP 1003LM), and a cryogenic pump (ULVAC CRUYO-U20PN). The two pump sets serve the instrument cabin and the sample cabin, respectively, and the whole vacuum pumping system is designed to be thoroughly oilless to prevent the target samples from contamination. The limit vacuum degree achievable in the cabin can reach 10^{-5} Pa level.

3.3. Temperature Control System

The temperature control system contains a heating system and a liquid nitrogen cooling system, distributed between the heat sink and the inner wall of the cabin, and underneath the cold plate. This mode allows the heating system and cooling system to be distributed around the instrument (MarSCoDe laboratory model) and samples, resulting in the uniform temperature for them. Based on the operation of the temperature control system, the cabin temperature can vary from -190 °C to +180 °C according to the actual demand. Temperature monitoring probes are distributed in different positions in both the instrument cabin and the sample cabin, and PID (proportion integral differential) algorithm is adopted to intelligently adjust the cabin temperature and ensure the temperature stability. The homogeneity of the temperature in the whole vacuum chamber can be evaluated by the standard deviation of the temperature data points measured by the different probes at a certain instant, with the standard deviation generally at 0.2 °C level.

3.4. Atmosphere Simulation System

The atmosphere simulation system consists of a gas filling and mixing unit and a quadrupole mass spectrometer. The gas filling and mixing is implemented by a gas injection pipeline including four parallel channels, meaning that up to four different kinds of gases can be injected into the cabin simultaneously and mixed in the cabin subsequently. Note that the gas injection pipeline itself would be pumped to high vacuum by the magnetic suspension molecular pump before the gas filling. The injection rate of each gas can be manipulated by a mass flowmeter, as demonstrated in Figure 5, hence the desired gas component proportion can be achieved.

Figure 5. The mass flowmeter for the manipulation of the injection rate of each kind of gas.

The quadrupole mass spectrometer (INFICON Transpector MPH300M) is used to monitor the gas component proportion of the mixed gas in real-time. When the quadrupole mass spectrometer works, its cavity should be in vacuum, and this is realized by the magnetic suspension molecular pump of the sample cabin.

3.5. Measurement and Control System

A computer central control unit with specific software systems is developed to visualize and manage the various parameters of the different modules in the whole facility.

To manage the vacuum degree parameters, different types of vacuum measuring instruments are exploited, including two compound vacuometers (INFICON VGC503), two low vacuum gauges (INFICON PSG500), four low/high vacuum compound ionization gauges (INFICON MPG400, INFICON BPG400), and two film gauges (INFICON CDG025D).

To manage the temperature parameters, we employ an intelligent temperature controller (ALTEC AL808) to monitor the operation status of the temperature control system in the instrument cabin and the third section of the sample cabin, and to inspect the real-time temperatures of the heaters and the liquid nitrogen pipelines. We also use two sets of multi-channel temperature inspection instruments to examine the temperatures of different modules of the MarSCoDe laboratory model. The accuracy of the temperature measurement and control can reach 0.1 °C level.

4. Verification of the Facility Technical Specifications

4.1. Vacuum Degree Testing

As mentioned in Section 3.2, two identical vacuum pump sets are deployed in this facility to serve the instrument cabin and the sample cabin, with different types of vacuum gauges measuring the vacuum degree in real time. When measuring the pressure in high level vacuum (less than 1 Pa), we used high vacuum compound ionization gauges (INFICON BPG400), with the accuracy being ±15% in the range of 10^{-6} to 1 Pa according to the official product manual. When measuring the pressure in mediate level vacuum (1 to 1000 Pa), we used high accuracy film gauges (INFICON CDG025D), with the accuracy being ±1.75 Pa at 876 Pa (simulated Martian environment) according to the official product manual.

In the vacuum degree testing, we inspected the vacuum performance of the whole device. For the chamber, the initial atmospheric condition was ordinary laboratory environment. The process of creating the vacuum environment consists of three stages. Firstly (15:00–16:30), a primary pumping was performed by the oilless dry pump to roughly discharge the gas in the gas pipe and cabin. When the pressure reached about 10 Pa, the magnetic suspension molecular pump also joined in and the secondary pumping started (two pumps worked together). The secondary pumping process went on in the subsequent 8 h or so (16:30–00:30), and the pressure slowly decreased from 10 Pa level to 1.25×10^{-3} Pa, which is the limit vacuum level that can be achieved by the magnetic suspension molecular pump. Finally, the tertiary pumping was activated at 00:30 (the cryogenic pump joined in), and all the three pumps jointly worked and the cabin pressure reached 10^{-5} Pa level about 11.5 h later (00:30–12:00). The temporal evolution curve of the vacuum degree is illustrated in Figure 6.

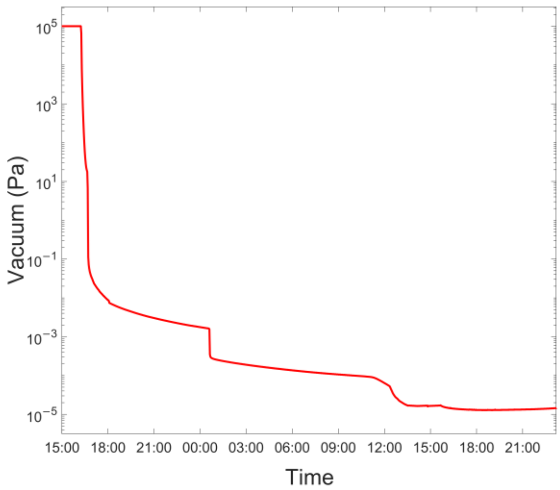

Figure 6. The temporal evolution curve of the vacuum degree in the facility.

The vacuum degree testing results demonstrate that the vacuum system of this facility is able to establish a vacuum environment, with the limit pressure reaching as low as 1.28×10^{-5} Pa. The high vacuum environment of the platform can meet the requirements for the simulation of the Martian surface atmosphere.

4.2. Temperature Testing

We have examined the temperature variation performance of the instrument cabin and the sample cabin, setting five temperature measuring points in the instrument cabin and two in the sample cabin. The practical value (PV) of the temperature at each point was monitored in real time, with the five values for the instrument cabin denoted as PV1 to PV5 and the two values for the sample cabin denoted as PV6 and PV7.

The mean and standard deviation of the seven PVs have been calculated to evaluate the accuracy of the temperature measurement. For the high temperature limit (180 °C), we chose the real-time PVs (at 21:16:23) when the temperature was at a stable level to perform the calculation. The mean is 180.1 °C and the standard deviation is 0.3 °C, indicating a very good accuracy of the cabin temperature measurement. For the low temperature limit (−190 °C), a similar strategy was adopted (at 13:32:53). The mean is −189.9 °C and the standard deviation is 3.2 °C, also indicating a good accuracy of the temperature measurement.

For the instrument cabin, under the no-load condition (i.e., neither the instrument nor the samples is placed in the chamber), it took about 60 min to raise the temperature from about 0 °C to the upper limit temperature 180 °C, and in the subsequent two to three hours, this temperature could be well maintained with an accuracy of about ±0.5 °C, as shown in Figure 7a. For the sample cabin, the general condition was identical, except that the temperature raising time was a bit longer, about 83 min, as shown in Figure 7b.

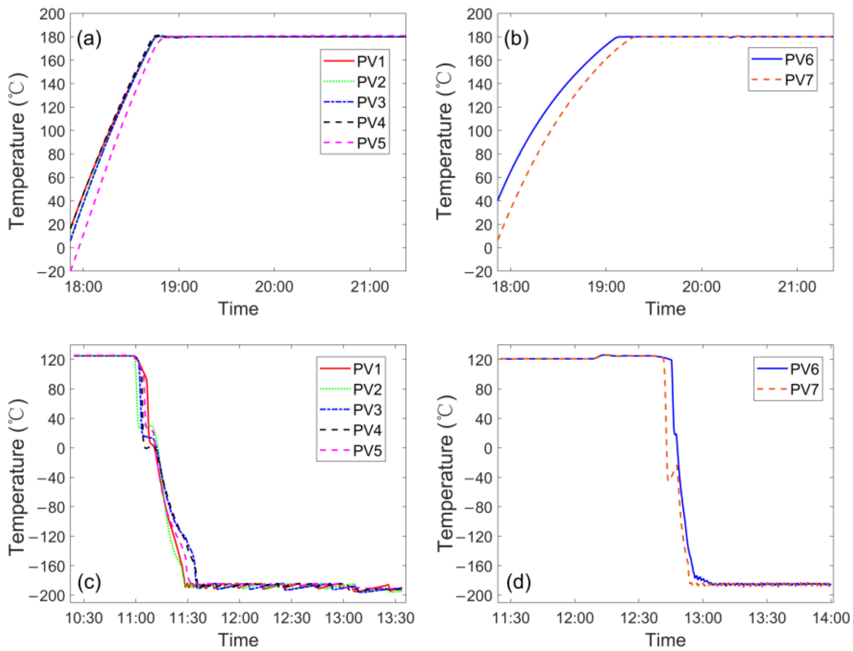

Figure 7. The temporal evolution curve of the temperature in the instrument cabin and the sample cabin. (**a**) Temperature raising process for the instrument cabin. (**b**) Temperature raising process for the sample cabin. (**c**) Temperature dropping process for the instrument cabin. (**d**) Temperature dropping process for the sample cabin.

For the instrument cabin, under the no-load condition, it took about 39 min to reduce the temperature from about 120 °C to the lower limit temperature −190 °C, and in the subsequent one to two hours, this temperature could be maintained with an accuracy of nearly ±2 °C, as shown in Figure 7c. For the sample cabin, the general condition was the same, except that the temperature dropped a bit faster, taking about 25 min, as shown in Figure 7d.

The temperature testing results indicate that the temperature control system of this facility can establish an environment with a temperature ranging from −190 °C to 180 °C, hence able to meet the demand for Martian environment simulation.

4.3. Gas Composition Testing

In this test, we employed a quadrupole mass spectrometer (INFICON Transpector MPH300M) to evaluate how well the gas composition in the Martian atmosphere is simulated. The cabin (either the instrument cabin or the sample cabin) was first pumped to vacuum condition, and then filled with a mixed gas simulating Martian atmosphere. The gas injection was implemented by the atmosphere simulation system described in Section 3.4. The preset gas component proportion of the mixture in this test was CO_2 95.73%, N_2 2.67%, and Ar 1.60%, and the total atmosphere pressure was 50 Pa. The actual achieved component proportion was then measured by the quadrupole mass spectrometer. The measurement result showed that the mixed gas composition was CO_2 96.00%, N_2 2.55%, and Ar 1.45%, indicating a mean relative error of approximately 0.2%.

The gas composition testing results have verified that the Martian atmospheric environment can be effectively simulated in this facility.

5. Preliminary Results of LIBS Experiments

5.1. Element Identification

The element identification ability of the MarSCoDe laboratory model has been examined. The test was conducted in an ordinary atmosphere, with a room temperature of 25 °C and a detection distance of 2.0 m. The target sample employed is a national reference material, namely a wollastonite (reference No. GBW03123), whose chemical composition is listed in Table 3 (in weight percentage).

Table 3. The main chemical components contained in the wollastonite sample (reference No. GBW03123). The content values are presented in weight percentage.

Component	SiO_2	CaO	MgO	Al_2O_3	FeO	K_2O
Content (wt.%)	50.5	40.39	0.95	0.39	0.28	0.14
Component	Fe_2O_3	MnO	Na_2O	P_2O_5	TiO_2	S
Content (wt.%)	0.1	0.096	0.052	0.052	0.022	0.01

The LIBS spectrometer unit of the MarSCoDe instrument consists of three spectral channels, covering 240–340 nm, 340–540 nm, and 540–850 nm, respectively [3], and this holds true for the MarSCoDe laboratory model. In Figure 8, a typical LIBS spectrum acquired from the wollastonite sample is shown, with the three subplots denoting the three spectral channels and the data represented by blue, green, and red lines, respectively. It is worth mentioning that the displayed spectrum has undergone a few preprocessing steps, including dark subtraction, noise filtering, baseline removal, and wavelength calibration.

Based on the NIST standard database [14], we identified the characteristic emission lines of several elements, namely Si, Ca, Mg, Al, K, Mn, Na, and O, covering the majority of the components contained in the wollastonite sample. A few elements could not be identified due to their too-low concentrations. The results shown in Figure 8 imply that the MarSCoDe laboratory model is able to provide physically reliable LIBS data.

5.2. Different Atmospheric Environments

In this investigation, LIBS spectra were collected in two different atmospheric environments. The first one is the normal atmospheric environment (25 °C), and the second one is a simulated Martian environment (−16 °C; 876 Pa; CO_2 95.73%, N_2 2.67%, Ar 1.6%). The recruited target sample was a Ti alloy, a duplicate of the Ti alloy standard on the calibration board of the Zhurong rover [3]. The target sample and MarSCoDe laboratory model were placed in the sample cabin and the instrument cabin of the platform, respectively, with the detection distance being 2.0 m in both LIBS measurements.

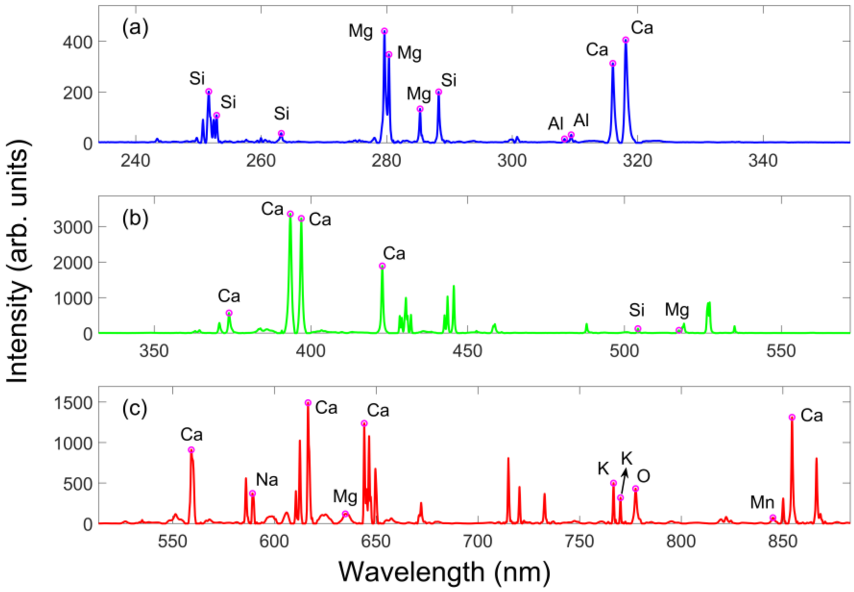

Figure 8. The LIBS spectrum collected from the wollastonite reference sample, in the ordinary laboratory environment. (**a**) The spectrum in Channel 1 (blue line). (**b**) The spectrum in Channel 2 (green line). (**c**) The spectrum in Channel 3 (red line). The identified characteristic peaks of several elements are marked out (magenta circles).

The LIBS spectra collected in the two environments are illustrated in Figure 9. The ordinary laboratory environment is denoted as environment 1 (Env1) and the spectra are presented by red lines, while the simulated Martian environment is denoted as environment 2 (Env2) and the spectra are indicated by blue dashed lines. The displayed spectra underwent the preprocessing steps described in Section 5.1.

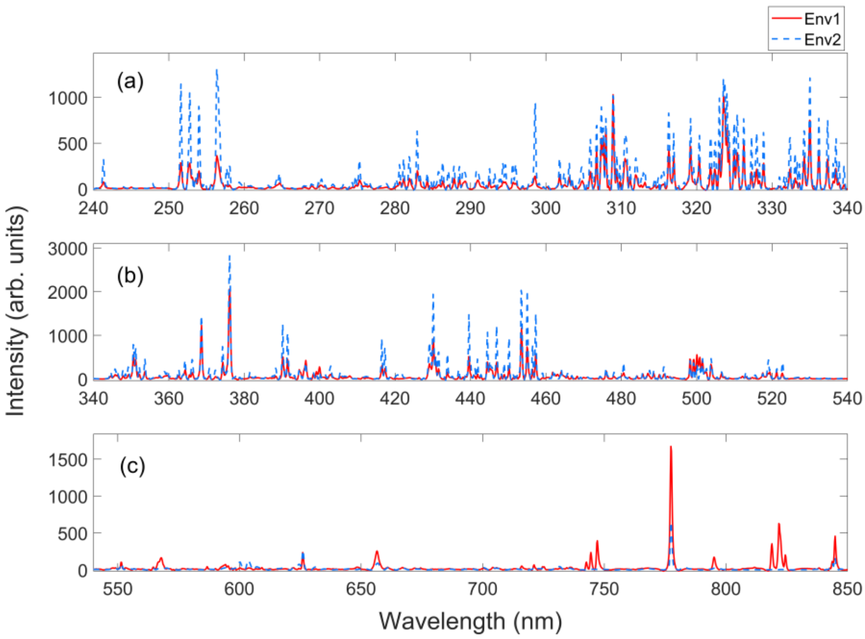

Figure 9. The LIBS spectra acquired from the Ti alloy reference sample in two different atmospheric environments. The red lines represent the result for environment 1 (Env1), and the blue dashed lines for environment 2 (Env2). (**a**) The spectra in Channel 1. (**b**) The spectra in Channel 2. (**c**) The spectra in Channel 3.

It should be emphasized that the wavelength–pixel correspondence is dependent on the experimental environment, indicating that the wavelength calibration result of the ordinary laboratory environment is not applicable to the simulated Martian environment. Specifically, for the ordinary environment, the wavelength calibration can be expressed by $\lambda = a^*x^2 + b^*x + c$, where λ represents the wavelength, x denotes the pixel serial number, and a, b, and c are instrument-dependent coefficients. When the environment changes, although a, b, and c are unaffected, an additional term Δx should be introduced, i.e., $\lambda = a^* (x + \Delta x)^2 + b^* (x + \Delta x) + c$. This term is not negligible since the temperature in the simulated Martian environment is considerably different from that in the ordinary environment. In fact, considerable wavelength drift can be observed in the two sets of LIBS data due to the significant temperature discrepancy between the two environments. Hence, in this test, a wavelength drift correction was conducted as an additional preprocessing step.

The spectra shown in Figure 9 are the results obtained after the wavelength drift correction. For each of the two LIBS datasets, the wavelength drift correction was carried out based on the comparison between the detected Ti emission lines and those lines recorded in the NIST database. The wavelength drift value was calculated for each of the three spectral channels individually. For each channel, about 20 Ti emission lines were selected and their drift values were calculated based on the NIST data. Finally, the mean of the drift values was employed as the overall drift value of the whole channel. In other words, within each spectral channel the wavelength drift correction value for each pixel is uniform, while the wavelength drift correction values of different channels are distinct. The Ti emission peaks of the two spectra can coincide well, implying that the MarSCoDe laboratory model can function competently in both environments, and that the wavelength drift correction scheme adopted herein is effective. Our results coincide with the conclusion presented in [10,15] that the emission line intensities of certain elements can be higher in the Martian atmospheric environment than in the normal ambient environment.

5.3. Different Detection Distances

For the field detection of MarSCoDe on Mars, the LIBS detection distance can hardly be kept constant. Thanks to the large volume of the facility and the long track inside the sample cabin, the LIBS detection distance can range from 1.5 m to 7 m, as mentioned in Section 3.1.

In this inspection, LIBS measurements were taken on another national reference material, namely a basalt sample (reference No. GBW7105). The experiment was implemented in the normal laboratory environment, with two different detection distances adopted, i.e., 2 m and 5 m.

The spectra collected at the two detection distances are shown in Figure 10, with the orange lines representing the result for 2 m and the purple lines for 5 m. It can be seen that the wavelength positions of the characteristic emission lines hardly change with the detection distance, while the intensities of the majority of the lines decrease when the distance is enlarged. These results are physically reasonable, indicating the validity of the LIBS data achieved by the MarSCoDe laboratory model.

5.4. Results of MarSCoDe and Its Laboratory Model in Simulated Martian Environment

Before the flight of the MarSCoDe instrument in 2020, we had collected quite a few LIBS spectra on the Ti alloy calibration standard in a simulated Martian environment (in 2019). In order to compare the performance of the MarSCoDe and its laboratory model, we reproduced the simulated environment with this platform, and collected LIBS spectra on the duplicate Ti alloy sample by MarSCoDe laboratory model. The simulated Martian environment herein and that in the pre-flight experiment have the same parameters as those described in Section 5.2. The detection distance is 3 m, identical to the distance in the pre-flight experiment. The spectra collected from MarSCoDe and its duplicate model are illustrated in Figure 11, and the results are also after preprocessing procedures. In addition to dark subtraction, wavelength drift correction, and wavelength calibration, the preprocessing herein also includes radiometric calibration and spectral normalization (normalized by the sum of the spectral intensities for each channel).

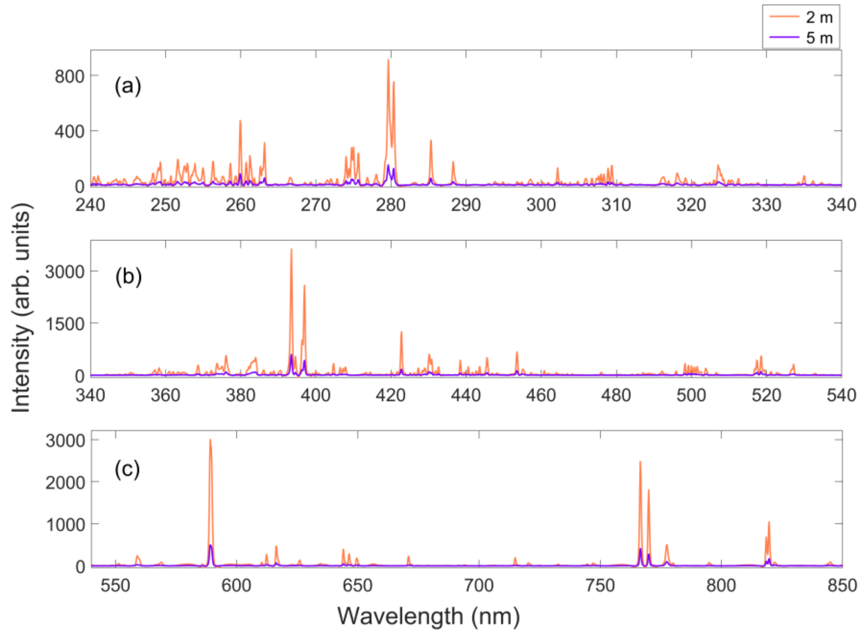

Figure 10. The LIBS spectra collected from the basalt reference sample at the two distances, in the ordinary laboratory environment. The orange lines denote the result for 2 m and the purple lines for 5 m. (**a**) The spectra in Channel 1. (**b**) The spectra in Channel 2. (**c**) The spectra in Channel 3.

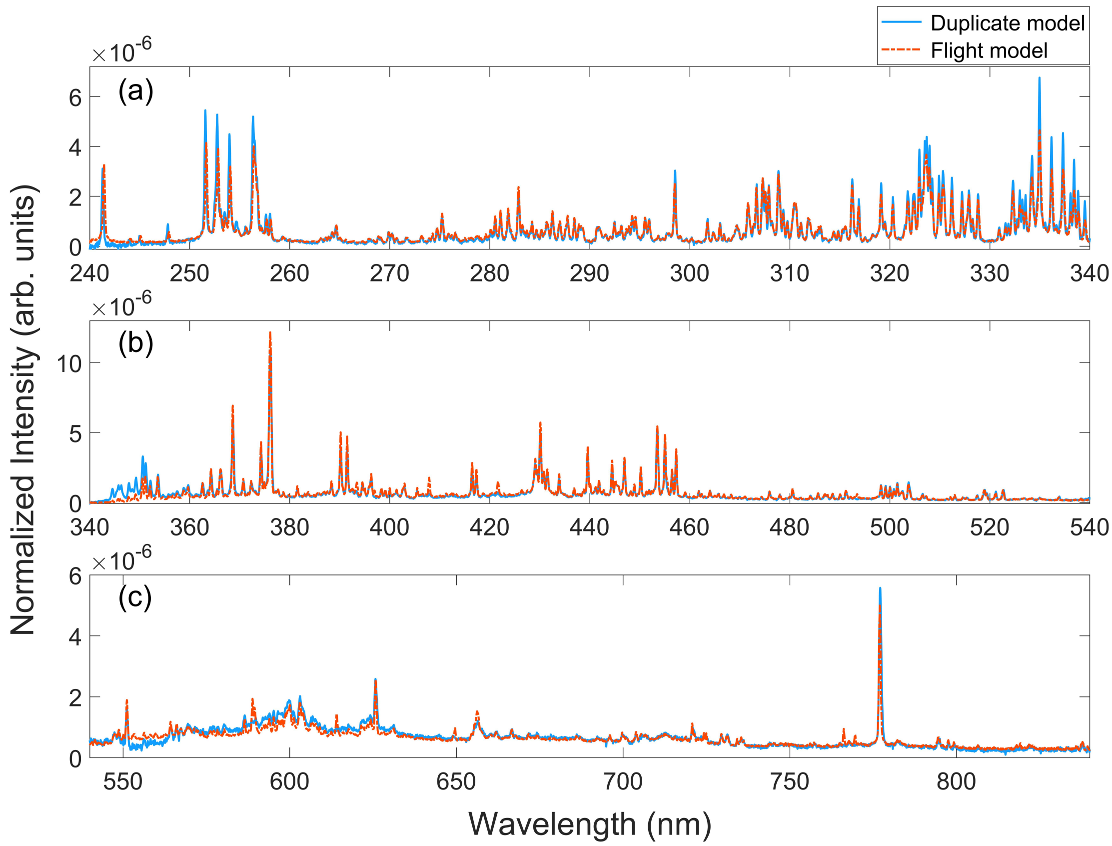

Figure 11. The LIBS spectra of a Ti alloy sample collected by the MarSCoDe flight model (red dashed lines) and the duplicate laboratory model (blue lines) in a simulated Martian environment. The detection distance is 3 m. (**a**) The spectra in Channel 1. (**b**) The spectra in Channel 2. (**c**) The spectra in Channel 3.

The profiles of these two spectra are highly similar despite the inconsistency in a few parts in the spectra. The slight discrepancies could originate from: (i) the slight deviations between MarSCoDe and its duplicate model in radiometric calibration; (ii) the tiny differences between the two simulated Martian environments, and the fact that the MarSCoDe instrument was outside the vacuum cabin (in ordinary atmosphere) in the pre-flight experiment; and (iii) the inherent fluctuations in the LIBS emission line intensities. The results demonstrate that the overall system functions of the two instruments are basically identical.

5.5. LIBS Spectra in Simulated Martian Environment and Field Detection on Mars

We have also analyzed the LIBS spectra of the Ti alloy sample collected by MarSCoDe laboratory model in the simulated Martian environment and the spectra of the Ti alloy standard acquired by MarSCoDe in the field detection (calibration) on Mars (sol 41 03:15:49). The spectra are demonstrated in Figure 12, and the spectral preprocessing procedures are the same as those stated in Section 5.4. As can be seen, the two sets of LIBS spectra coincide well, indicating that a high-degree simulation of MarSCoDe field detection on Mars can be achieved in our platform.

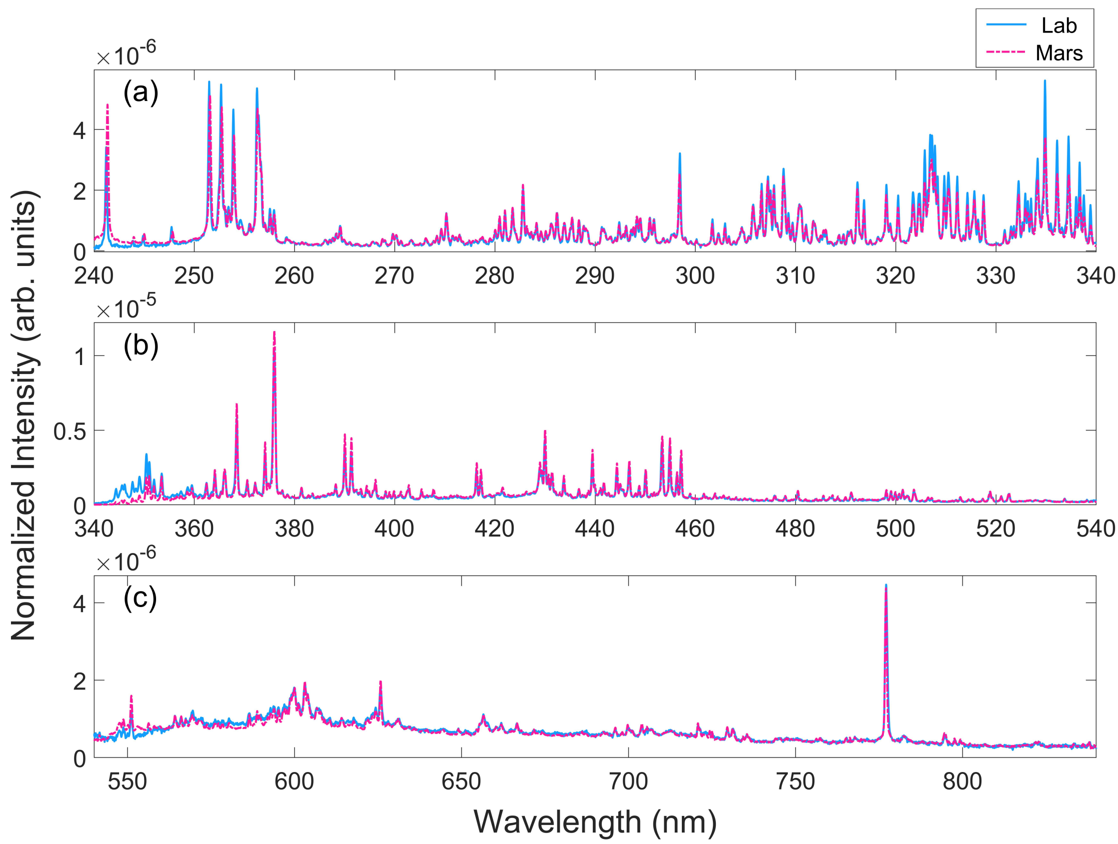

Figure 12. The LIBS spectra collected by MarSCoDe in field detection (calibration) on Mars (purple dashed lines) and by the MarSCoDe laboratory model in the simulated Martian environment (blue lines), with the targets being two identical Ti alloy samples. (**a**) The spectra in Channel 1. (**b**) The spectra in Channel 2. (**c**) The spectra in Channel 3.

5.6. Future Work

This paper only presents some preliminary results of the implemented LIBS experiments in the facility. Utilizing the MarSCoDe laboratory model and the remarkable simulated Martian environment, we will carry out more LIBS experiments to simulate the MarSCoDe in situ detection on Mars, and a large-scale LIBS database is expected to be established. In addition, more in-depth LIBS qualitative and quantitative analysis will be conducted based on the database. In addition to the conventional LIBS chemometrics such as principal component analysis [16] and partial least squares [17], more modern machine learning methods will be exploited, such as the diverse artificial neural network-based methods, especially the state-of-art deep learning techniques such as convolutional neural network [18,19]. The studies conducted based on this platform are expected to play a critical role in the interpretation of the MarSCoDe LIBS data in the future.

6. Conclusions

In this paper, we have introduced a LIBS experiment platform located in Hangzhou, China, which is able to simulate the Martian atmospheric environment. In the simulated environment, the limit vacuum degree can reach 10^{-5} Pa level, the temperature can vary from -190 °C to +180 °C, and different kinds of gases can be filled and mixed at an adjustable proportion. The most distinctive advantage of this facility is that, aside from the target samples, the LIBS instrument can also be placed into the simulated environment. Moreover, the laser-target distance can be flexibly modulated within a range of 1.5 m to 7 m.

The LIBS instrument employed in this platform is a duplicate model of the MarSCoDe flight model launched in Tianwen-1 mission, and the system constitution and technical parameters of the MarSCoDe instrument have been briefly presented. In addition, we have elaborated the architecture of the facility, i.e., a vacuum chamber (including an instrument cabin, a sample cabin, a sample import chamber, and a 3D vacuum stage), a vacuum pumping system, a temperature control system, an atmosphere simulation system, a measurement and control system, and other auxiliary devices. The performance specifications regarding vacuum degree, temperature, and gas composition have been validated through specifically designed examinations.

A series of LIBS experiments have been carried out and some of the preliminary results are demonstrated, including the verification of the element identification ability, the comparison of LIBS spectra collected in the ordinary laboratory environment and the simulated Martian environment, the comparison of LIBS spectra detected at different distances, and the comparison of LIBS spectra acquired by the MarSCoDe flight model and the duplicate laboratory model.

The results indicate that the LIBS experiment platform can realize a high-degree simulation of the actual scenario of MarSCoDe field detection on Mars. Based on this platform, a large-scale LIBS database is expected to be established, and more in-depth data retrieval work will be implemented, hence offering data support for the accurate and efficient analysis of the MarSCoDe in-situ LIBS data in the future.

Author Contributions: Conceptualization, X.X., L.J. and Z.C.; formal analysis, L.L.; methodology, X.L. and W.X.; supervision, R.S.; writing—original draft, Z.C.; writing—review and editing, L.L. and X.X. All authors have read and agreed to the published version of the manuscript.

Funding: This work was supported by National Natural Science Foundation of China (No. 11904378), Key Laboratory of Lunar and Deep Space Exploration, CAS (No. LDSE201802, LDSE202003), Key Laboratory of Space Active Opto-Electronics Technology, Shanghai Institute of Technical Physics (No. 2021-ZDKF-2), and Natural Science Foundation of Shanghai (No. 22ZR1472400).

Data Availability Statement: Not applicable.

Conflicts of Interest: The authors declare no conflict of interest.

References

1. Wu, X.; Liu, Y.; Zhang, C.L.; Wu, Y.C.; Zhang, F.; Du, J.; Liu, Z.H.; Xing, Y.; Xu, R.; He, Z.P.; et al. Geological characteristics of China's Tianwen-1 landing site at Utopia Planitia, Mars. *Icarus* **2021**, *370*, 16. [CrossRef]
2. Shu, R.; Xu, W.; Fu, Z.; Wan, X.; Yuan, R. Laser Induced Breakdown Spectroscopy Detector in Deep Space Exploration. *J. Deep Space Explor.* **2018**, *5*, 450–457. (In Chinese)
3. Xu, W.M.; Liu, X.F.; Yan, Z.X.; Li, L.N.; Zhang, Z.Q.; Kuang, Y.W.; Jiang, H.; Yu, H.X.; Yang, F.; Liu, C.F.; et al. The MarSCoDe Instrument Suite on the Mars Rover of China's Tianwen-1 Mission. *Space Sci. Rev.* **2021**, *217*, 58. [CrossRef]

4. Zou, Y.; Zhu, Y.; Bai, Y.; Wang, L.; Jia, Y.; Shen, W.; Fan, Y.; Liu, Y.; Wang, C.; Zhang, A.; et al. Scientific objectives and payloads of Tianwen-1, China's first Mars exploration mission. *Adv. Space Res.* **2021**, *67*, 812–823. [CrossRef]
5. Morgenstern, A.; Hauber, E.; Reiss, D.; Van Gasselt, S.; Grosse, G.; Schirrmeister, L. Deposition and degradation of a volatile-rich layer in Utopia Planitia and implications for climate history on Mars. *J. Geophys. Res. Planet* **2007**, *112*, 11. [CrossRef]
6. Ulrich, M.; Morgenstern, A.; Gunther, F.; Reiss, D.; Bauch, K.E.; Hauber, E.; Rossler, S.; Schirrmeister, L. Thermokarst in Siberian ice-rich permafrost: Comparison to asymmetric scalloped depressions on Mars. *J. Geophys. Res. Planet* **2010**, *115*, 22. [CrossRef]
7. Kieffer, H.H. Soil and surface temperatures at viking landing sites. *Science* **1976**, *194*, 1344–1346. [CrossRef] [PubMed]
8. Hess, S.L.; Ryan, J.A.; Tillman, J.E.; Henry, R.M.; Leovy, C.B. The annual cycle of pressure on mars measured by viking-lander-1 and viking-lander-2. *Geophys. Res. Lett.* **1980**, *7*, 197–200. [CrossRef]
9. Sobron, P.; Wang, A. A planetary environment and analysis chamber (PEACh) for coordinated Raman-LIBS-IR measurements under planetary surface environmental conditions. *J. Raman Spectrosc.* **2012**, *43*, 212–227. [CrossRef]
10. Cousin, A.; Forni, A.; Maurice, S.; Gasnault, O.; Fabre, C.; Sautter, V.; Wiens, R.C.; Mazoyer, J. Laser induced breakdown spectroscopy library for the Martian environment. *Spectrochim. Acta Part B At. Spectrosc.* **2011**, *66*, 805–814. [CrossRef]
11. Wu, Z.C.; Ling, Z.C.; Zhang, J.; Fu, X.H.; Liu, C.Q.; Xin, Y.Q.; Li, B.; Qiao, L. A Mars Environment Chamber Coupled with Multiple In Situ Spectral Sensors for Mars Exploration. *Sensors* **2021**, *21*, 2519. [CrossRef]
12. Sears, D.W.G.; Benoit, P.H.; McKeever, S.W.S.; Banerjee, D.; Kral, T.; Stites, W.; Roe, L.; Jansma, P.; Mattioli, G. Investigation of biological, chemical and physical processes on and in planetary surfaces by laboratory simulation. *Planet. Space Sci.* **2002**, *50*, 821–828. [CrossRef]
13. Martin-Gago, J.A.; Mateo-Marti, E.; Gomez, F.; Prieto Ballesteros, O.; Gomez Elvira, J. A chamber for studying planetary environments and its applications to astrobiology. *Astrobiology* **2006**, *6*, 252.
14. Ralchenko, Y.; Kramida, A. Development of NIST atomic databases and online tools. *Atoms* **2020**, *8*, 56. [CrossRef] [PubMed]
15. Brennetot, R.; Lacour, J.L.; Vors, E.; Rivoallan, A.; Vailhen, D.; Maurice, S. Mars analysis by laser-induced breakdown spectroscopy (MALIS): Influence of mars atmosphere on plasma emission and study of factors influencing plasma emission with the use of Doehlert designs. *Appl. Spectrosc.* **2003**, *57*, 744–752. [CrossRef] [PubMed]
16. Porizka, P.; Klus, J.; Kepes, E.; Prochazka, D.; Hahn, D.W.; Kaiser, J. On the utilization of principal component analysis in laser-induced breakdown spectroscopy data analysis, a review. *Spectrochim. Acta Part B At. Spectrosc.* **2018**, *148*, 65–82. [CrossRef]
17. Xu, X.; Liu, J.; Liu, D.; Liu, B.; Shu, R. Photometric Correction of Chang'E-1 Interference Imaging Spectrometer's (IIM) Limited Observing Geometries Data with Hapke Model. *Remote Sens.* **2020**, *12*, 3676. [CrossRef]
18. Li, L.N.; Liu, X.F.; Xu, W.M.; Wang, J.Y.; Shu, R. A laser-induced breakdown spectroscopy multi-component quantitative analytical method based on a deep convolutional neural network. *Spectrochim. Acta Part B At. Spectrosc.* **2020**, *169*, 18. [CrossRef]
19. Li, L.N.; Liu, X.F.; Yang, F.; Xu, W.M.; Wang, J.Y.; Shu, R. A review of artificial neural network based chemometrics applied in laser-induced breakdown spectroscopy analysis. *Spectrochim. Acta Part B At. Spectrosc.* **2021**, *180*, 18. [CrossRef]